A comparison of global motion perception using a multiple-aperture stimulus

Alan L. F. Lee

Department of Psychology, University of California, Los Angeles, CA, USA

Hongjing Lu

Department of Psychology, University of California, Los Angeles, CA, USA, &
Department of Statistics, University of California, Los Angeles, CA, USA

The human visual system integrates local motion signals to generate globally coherent motion percepts. However, it is unclear whether the perception of different types of global motion relies on a common motion integration mechanism. Using the multiple-aperture stimulus developed by K. Amano, M. Edwards, D. R. Badcock, and S. Nishida (2009), we compared the motion sensitivity (in terms of coherence threshold) for translational, circular, and radial motion. We found greater motion sensitivity for the two complex (circular and radial) motion types than for translational motion, implying that specific motion integration mechanisms are involved in the computation for different motion types. Our results reveal a "complexity advantage" in perceiving motion, which is consistent with physiological and computational evidence suggesting that specific mechanisms exist for processing complex circular/radial motion. We further examined the contributions of several critical factors that influence human global motion sensitivity. We found that human sensitivity for all motion types remained constant across a range of motion sampling density but varied depending on global speed. The minimum stimulus duration required for observers to reach constant sensitivity was found to be short (~140 ms) for all motion types.

Keywords: motion integration, global motion, optic flow, aperture problem

Citation: Lee, A. L. F., & Lu, H. (2010). A comparison of global motion perception using a multiple-aperture stimulus. *Journal of Vision, 10*(4):9, 1–16, http://journalofvision.org/10/4/9/, doi:10.1167/10.4.9.

Introduction

Imagine that you are traveling on a boat and viewing the moving water through a mesh railing with many holes. Through each hole, you can see the water drifting in different directions. Given these sampled motion signals projected onto the retina, your visual system can readily infer the global motion of the scene, determining, for example, whether the boat is moving forward or backward as well as the speed of the boat's movement. However, this task is far from trivial due to the inherent ambiguity of motion stimuli, usually termed the "aperture problem." As illustrated in Figure 1, when only a line segment of a moving object is viewed through a small aperture with the segment's end-points or terminators occluded, there are an infinite number of possible interpretations of the true motion of the object behind this aperture. One way to overcome the local ambiguity inherent in the visual dynamic stimulus is to integrate motion signals viewed from multiple apertures to infer the "true" velocity field for the occluded object.

Physiological evidence suggests that motion integration depends on a hierarchical motion processing network in the visual cortex. Directional-selective neurons in the primary visual cortex (V1) are sensitive to the motion energy within small receptive fields (Emerson, Bergen, & Adelson, 1992), which are used to estimate local motion. These local estimates are pooled in higher-level visual areas where neurons with large receptive fields are sensitive to global motion patterns. These global motion detectors include neurons in the middle temporal (MT) area (Britten, Shadlen, Newsome, & Movshon, 1993; Rust, Mante, Simoncelli, & Movshon, 2006) and in the medial superior temporal (MST) area (Duffy & Wurtz, 1991; Tanaka & Saito, 1989). This hierarchical system for processing motion has been supported by psychophysical studies (Morrone, Burr, & Vaina, 1995) and simulated by computational models (Heeger, Simoncelli, & Movshon, 1996).

However, although researchers generally agree that an integration stage is involved in motion processing, it remains unclear whether a common integration mechanism could underlie perception of optic flows viewed in everyday life. Researchers have proposed that the visual system could decompose optic flows into three cardinal components: translational, circular, and radial motion (e.g., Burr, Badcock, & Ross, 2001). These three basic motion patterns can jointly represent many kinds of real-world optic flows, generated from moving objects, from

doi: 10.1167/10.4.9 Received June 30, 2009; published April 22, 2010 ISSN 1534-7362

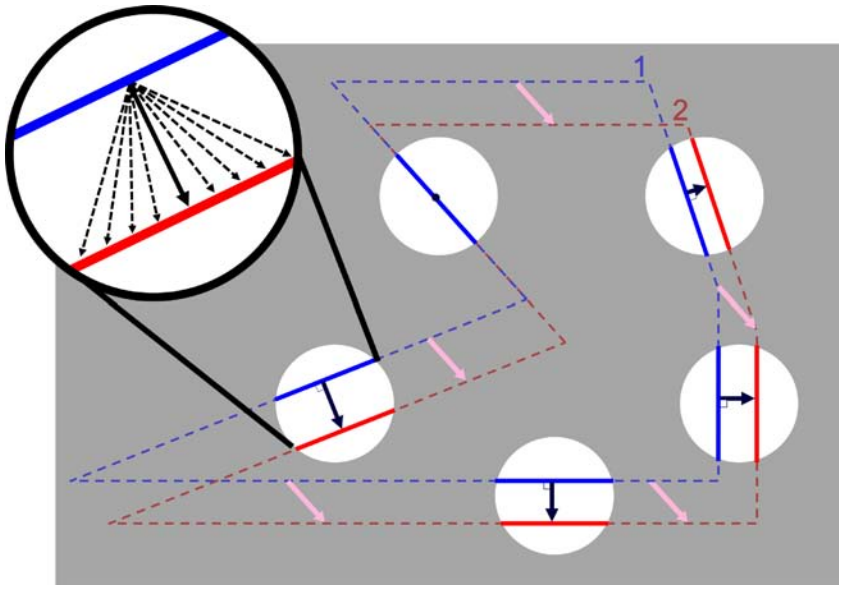

Figure 1. Illustration of the aperture problem. As a rigid object moves from Position 1 (blue outline) to Position 2 (red outline) with a down-rightward motion (pink arrows), each edge, when viewed through an aperture (white circle), is observed to move in the direction (dark blue arrows) orthogonal to its orientation. As shown in the magnified aperture, with only one local motion observed (thick solid arrow), the number of possible interpretations of the true motion of the whole object (thin dashed arrows) is infinite.

saccadic eye movements, and from ego-motion. Accordingly, detectors that are sensitive to these cardinal patterns can work cooperatively to represent a large range of optic flows. Circular and radial motions are often referred to as "complex" motions (Beardsley & Vaina, 2005; Bex, Metha, & Makous, 1999; Burr & Santoro, 2001; Clifford, Beardsley, & Vaina, 1999) because local motion vectors in rotation and expansion change with their locations, whereas local motion vectors in translation are constant over different spatial locations.

A few studies have aimed to compare human sensitivity in perceiving translational, circular, and radial motion in order to understand how the visual system conducts a global motion analysis on these motion patterns. However, results for comparisons over the three motion patterns have been inconsistent. The fundamental disagreement focuses on whether the visual system shows similar sensitivity to all three motion patterns or not. Some findings suggest that motion sensitivity for all three patterns is comparable. Blake and Aiba (1998) used high-contrast and low-density random-dot kinematogram (RDK) to measure motion sensitivity. For both motion detection and direction discrimination tasks, no significant difference was found in motion sensitivity measured with coherence thresholds across the three motion patterns. Other researchers used first-order (luminance-defined) motion stimuli of the RDK type and found that both contrast and coherence sensitivity for the three motion types were comparable (Aaen-Stockdale, Ledgeway, & Hess, 2007; Bertone & Faubert, 2003). On the other hand, various studies have reported the opposite results, finding that sensitivity differs across translational, circular, and radial motions. In an early study with RDK stimuli by Freeman and Harris (1992), detection thresholds were measured to quantify the minimum motion needed to detect a global motion pattern. They found that circular and radial motions yielded lower detection thresholds than did translational motion, indicating that the visual system is more sensitive to complex motion. Edwards and Badcock (1993) added a speed gradient into radial motion patterns and found higher motion sensitivity for centripetal patterns (simulating contracting optic flows during backward self-motion) than centrifugal (simulating expanding optic flow during forward self-motion) and frontoparallel (translational) motion. However, studies using second-order (texture-defined) motion represented by RDK stimuli (Bertone & Faubert, 2003) found that observers were more sensitive in perceiving translational motion than complex motion patterns (i.e., circular and radial motions). A similar pattern of results was also reported in a study with stimuli requiring segregation of motion structure (Ahlstrom & Borjesson, 1996).

Most of the previous studies of motion integration have used random-dot kinematogram (RDK) as the experimental stimulus. A potential problem with using dot stimuli to study motion integration is that the observer might track the trajectory of a few signal dots in the display to infer the global motion direction. To discouraging this local-tracking strategy, researchers use the limited lifetime technique with dot stimuli. However, this method does not completely rule out the tracking contribution if dot lifetime is more than two frames, or if the displacement of signal dot movement is small, or if signal dot movements can be easily segmented from noise dot movements.

Furthermore, an inevitable consequence of introducing limited lifetime to dot stimuli is that it interferes with temporal smoothness, which could ultimately affect observer's sensitivity in perceiving global motion. Given these possible drawbacks, RDK stimuli may not be the ideal stimulus type for studying motion integration.

An alternative motion stimulus is an array of sinusoidal gratings, or lines with different orientations (Amano, Edwards, Badcock, & Nishida, 2009; Mingolla, Todd, & Norman, 1992). Due to the aperture problem, the local velocity of each motion element is ambiguous when viewed individually. However, a coherent motion percept can be formed if the visual system processes motion information globally. This multiple-aperture stimulus can preclude local tracking and maintain temporal smoothness (as the Gabor gratings drift continuously) so as to amplify the use of sensitivity as a good measure of spatial integration. In addition, the multiple-aperture stimulus provides an effective tool for controlling the amount of information available at each element location, making it possible to tease apart different pooling mechanisms. For example, using the multiple-aperture stimulus, Amano et al. (2009) found that the human visual system employs different pooling strategies adaptively depending on the ambiguity in the local motion signals. However, all stimuli in their study were translational motion. It is therefore unclear whether and how the human visual system could perceive global complex motion patterns, such as circular and radial motion, when viewing these multiple-aperture stimuli.

To understand the mechanisms of motion integration, we employed the multiple-aperture stimulus to compare human sensitivity for three basic global motion patterns: translational, circular, and radial motion. We also investigated the characteristics of the motion integration mechanism for each specific motion pattern and examined the contributions of several factors that influence human global motion sensitivity. In the present paper we report three experiments. Experiment 1 was designed to compare motion sensitivity for translational, circular, and radial motion over a large range of spatial density of local motion signals. Experiment 2 aimed to study the change of human motion sensitivity as a function of speed for each global motion pattern. Finally, Experiment 3 examined the time course of motion integration mechanisms for specific motion patterns.

Multiple-aperture stimulus

We adopted the stimulus created by Amano et al. (2009), who defined two terms "1D motion" and "2D motion" for the purpose of stimulus description. The 1D motion (also termed "component motion") of a Gabor element refers to the drifting velocity of the element (as it can only drift in one single dimension orthogonal to the grating orientation). The 2D motion refers to the underlying true motion of the object behind apertures. For example, in Figure 1, the dark blue solid arrow in each aperture indicates the 1D motion of the drifting grating, whereas the thick pink arrows indicate the 2D motion of the whole object. The 1D motion corresponds to observations obtained from each element from the multiple-aperture stimulus, and the 2D motion is what observers need to infer about the true motion flow. To generate a multiple-aperture stimulus, the 1D motion of each Gabor element was computed based on its orientation and preassigned 2D motion direction.

The multiple-aperture stimulus consisted of 728 drifting Gabor elements arranged in a circular pattern inscribed in a 31 × 31 grid (as shown in Figure 2). Each Gabor element was an oriented sinusoidal grating windowed by a stationary Gaussian function. The spatial frequency of each grating was 5.58 cycles/deg and the standard deviation of the Gaussian window was 0.08 deg. Each Gabor element subtended a visual angle of 0.40 deg. The

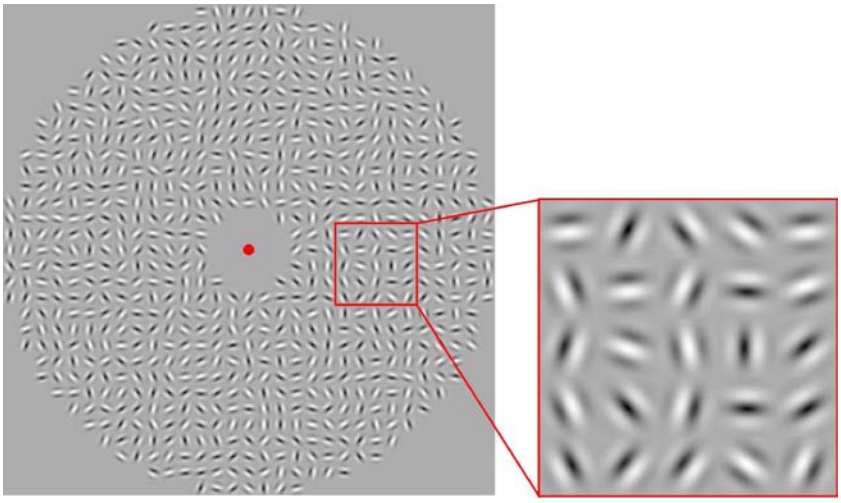

Figure 2. Screen shot of a typical stimulus instance and a zoomed view of the Gabor elements.

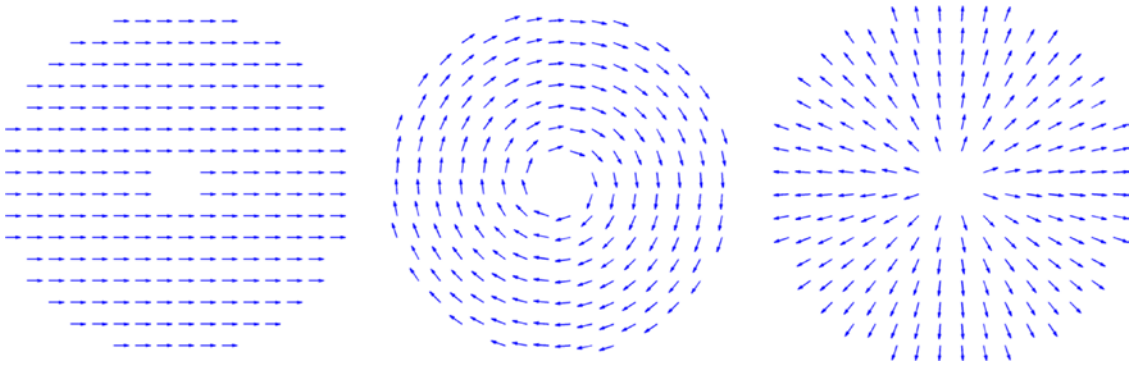

Figure 3. Schematic illustration of the three global motion patterns. Shown are three instances of motion patterns: rightward translational (left), clockwise circular (middle), and radially expanding motion (right). Arrows indicate the 2D motion vectors of the elements.

distance between the centers of two neighboring elements was 0.40 deg. The stimulus was displayed within a circular area of diameter 12.15 deg. There was a small, blank circular region with diameter subtending 1.96 deg at the center of the display window. A red fixation dot was located at the center of the display. Contrast for all Gabor elements were set at 0.4. Orientation of each Gabor element was randomly assigned in each trial.

The three global motion patterns (translational, circular, and radial motion) were created by manipulating 2D motion of Gabor elements. For translational motion, the 2D motion directions of all elements were the same (either rightward or leftward). For circular and radial motion, the 2D motion direction of each element was determined by its position relative to the center so that the pattern could be set to rotate around the center for circular motion (clockwise or counter-clockwise) or contract/expand relative to the center (inward or outward). Note that the speed of 2D motion was constant for all elements (implying non-rigid rotation and expansion/contraction

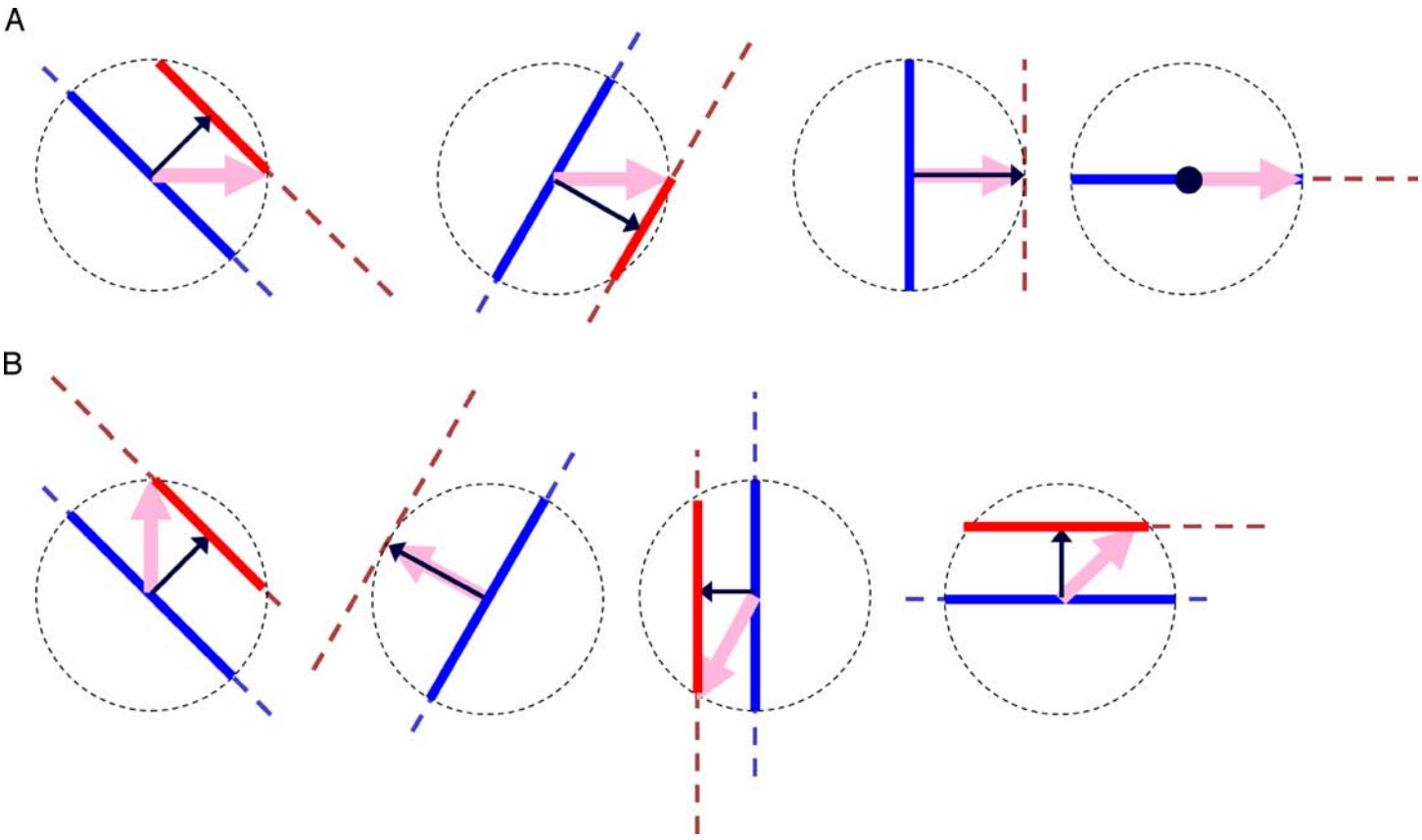

Figure 4. Diagram of (A) signal elements and (B) noise elements. Thick pink arrows indicate 2D motion. Thin dark blue arrows indicate 1D motion. Same convention as used in Figure 1.

for complex motion), so as to be compatible with speeds in translational motion. Figure 3 illustrates the three global motion patterns used in this study.

As shown in Figure 4, each Gabor element was categorized as either a signal or a noise element. For signal elements (see Figure 4A), the 2D motion was assigned as described in Figure 3, so that 2D motion for these signal elements represented a globally coherent motion pattern (translational, circular, or radial motion). For noise elements, the 2D motion directions were randomized while keeping the same speed (Figure 4B). For both signal and noise elements (regardless of the motion pattern), the 2D motion speed was kept constant at 0.79 deg/s (except for Experiment 2).

Strength of global motion was controlled by coherence ratio, which was defined as the proportion of signal elements among the total number of elements in the stimulus. As shown in movie examples (see Figure 5), a stimulus with 100% coherence ratio would have all the elements as signals, whereas a stimulus with 75% coherence ratio would have 75% of the elements as signals while the remaining 25% were noise elements.

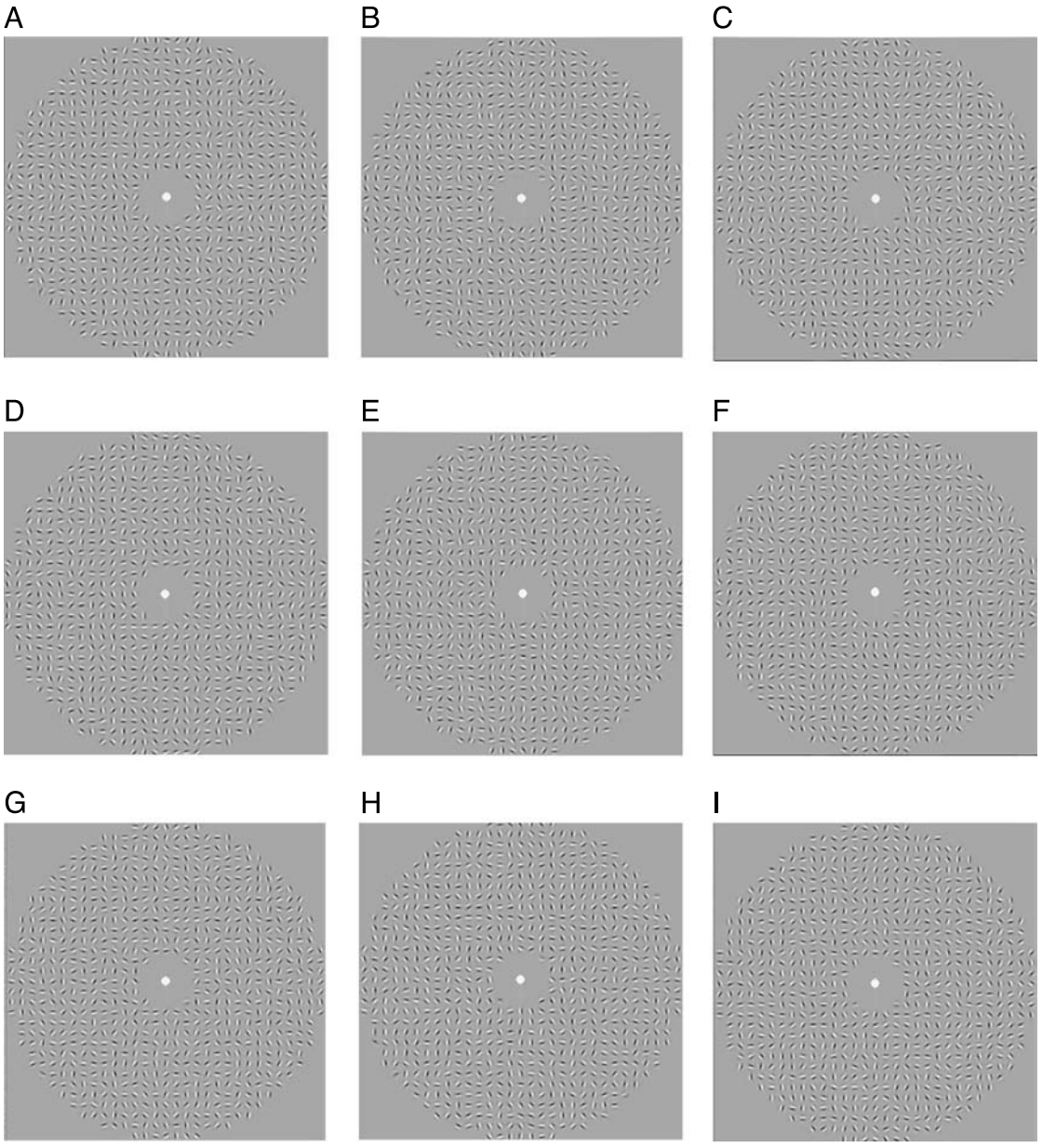

Figure 5. Multiple-aperture stimuli with different coherence ratios, including 100% (left column 5a, 5d, 5g), 75% (middle column 5b, 5e, 5h), and 20% (right column 5c, 5f, 5i). Each row includes motion stimuli for one type of motion pattern: translational (top row), circular (middle row), and radial motion (bottom row). Stimulus contrast was increased for the purpose of clear illustration. Fixation dot was red (instead of white as shown here) in the real stimulus.

Experiment 1: Comparing human sensitivity for translational, circular, and radial motion

Experiment 1 aimed to compare motion sensitivity in perceiving translational, circular, and radial global motion using the multiple-aperture motion stimulus. If specific motion integration mechanisms operated for different motion types, we would expect to find variation of human sensitivity for different motion types. A second goal of this experiment was to examine the integration characteristics in terms of the range of spatial pooling. The spatial extent of motion integration has been studied extensively using random-dot kinematograms (RDK). Several studies using the RDK stimuli demonstrated that human sensitivity for perceiving global translation remains nearly constant when dot density is doubled (Edwards & Badcock, 1994, 1995, 1996), as well as when dot density varies over a relatively large range (Barlow & Tripathy, 1997). This density invariance effect was also found in complex motion, i.e., circular (Morrone et al., 1995) and radial motion (Badcock & Khuu, 2001) using the RDK stimuli. Barlow and Tripathy (1997) provided a theoretical explanation of these findings using the ideal observer approach, which employs a linear pooling strategy within the display area to overcome the uncertainty induced by the correspondence problem inherent in the RDK stimuli. If a linear pooling strategy is a general integration mechanism adopted by the human visual system, we would expect the density invariance effect would be obtained using distinctly different motion stimuli. Accordingly, in Experiment 1 we measured motion sensitivity as a function of element density using the multiple-aperture stimulus, setting the size of the visual field to a value comparable to those used in previous studies with RDK stimuli.

Methods

Subjects

Fifteen undergraduate students from the University of California, Los Angeles (UCLA), participated in the experiment for course credit. The observers were naïve to the purpose of the experiment. All observers had normal or corrected-to-normal visual acuity. Five observers were randomly assigned to one of the three conditions: translational, circular, and radial motion.

Apparatus

Motion stimuli were presented on a Viewsonic CRT monitor with a refresh rate of 75 Hz and resolution of 1024 × 768 pixels, with a constant viewing distance of 57 cm using a chin rest. Each pixel on the screen subtended 2.01 arcmin. A Minolta CS-100 photometer was used to calibrate the monitor. A luminance range of 0–146.5 cd/m^2 was converted into a linear lookup table for 256 programmable intensity levels. Experiments were run in a dim room. Matlab and PsychToolbox (Brainard, 1997; Pelli, 1997) were used to present the stimuli.

Stimulus

The stimuli were similar to those described in the Multiple-aperture stimulus section, except for the spatial density. Different numbers of elements were presented at different levels of spatial density. We used seven density levels: 0.64, 1.29, 1.93, 2.58, 3.22, 4.84, and 6.45 elements/deg^2 (corresponding to 10%, 20%, 30%, 40%, 50%, 75%, and 100% of 728 elements, respectively, shown in the display window). As depicted in Figure 6, Gabor elements were confined in a circular window but the positions of presented elements were randomly selected from trial to trial on the fixed grid.

On each trial, the motion sequence consisted of 20 frames with frame duration of 13.33 ms per frame. Observers were told to fixate the red dot throughout the experiment. The fixation spot was presented for 500 ms and followed with the motion stimulus for 267 ms. After the motion stimulus disappeared from the screen, observers were asked to press one of two keys to respond. Observers' task was to identify the global direction from two alternative directions for each motion type: left/right for translational, clockwise/counter-clockwise for circular,

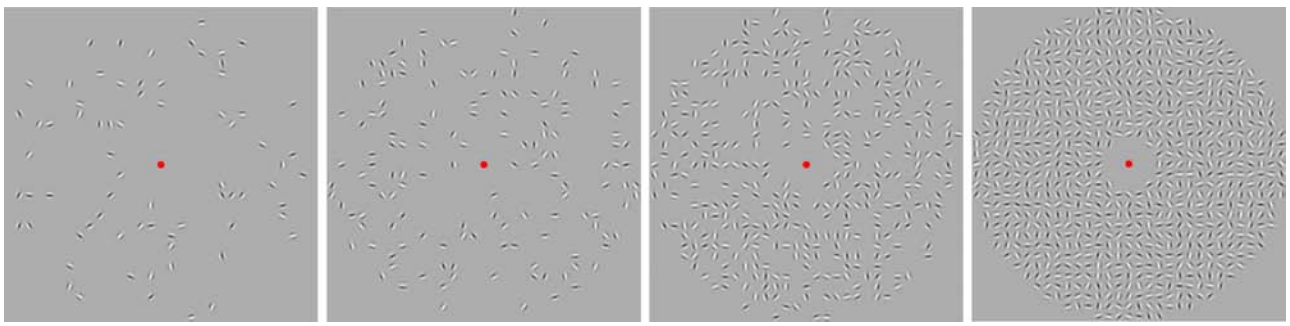

Figure 6. Stimuli of different densities used in Experiment 1. Examples illustrate four fixed levels of density of elements: (from left to right) 0.64 (10%), 1.29 (20%), 3.22 (50%), and 6.45 (100%) elements/deg^2.

and inward/outward for radial motion. The key-pressing response triggered the start of the next trial after 1 second.

Procedure

Seventy practice trials were administered to observers prior to each experiment session in order to familiarize them with the stimulus and the task. Coherence ratio was set to decrease during the practice, from 100% (first fourteen trials) to 80% (next seven trials), and then to 40% (the remaining 49 trials), so that observers could experience the different levels of task difficulty used in this experiment. After the practice, one experiment session was conducted, which included only one of the three types of motion (translational, circular, or radial). In both practice and experiment sessions, the presentation order of the seven different density levels was randomized over trials. Within an experiment session, coherence ratio for each density level was independently adjusted to achieve 75% accuracy using the QUEST adaptive-staircase procedure (Watson & Pelli, 1983), so that coherence thresholds for the seven density levels could be estimated independently (150 trials for each level) and served as the motion sensitivity measurement. In every trial of both practice and experiment sessions, a beep was played to provide negative feedback whenever participants made an error.

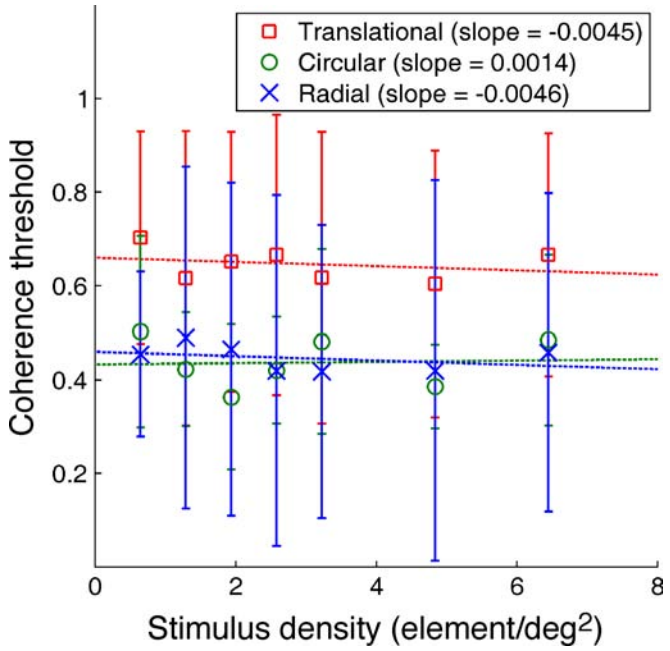

Figure 7. Results of Experiment 1. Coherence thresholds as a function of stimulus density for three motion patterns. Coherence thresholds (averaged across observers) are plotted across difference density levels for translational (red open squares), circular (green open circles), and radial (blue crosses) motion. For each motion type, the dotted line was fitted with averaged thresholds. Error bars show the 95% confidence intervals for the estimates of the means.

Results and discussion

As shown in Figure 7, the coherence threshold for translational motion was higher than that for circular/radial motion. High coherence thresholds indicate low sensitivity (i.e., worse performance in global motion perception). This result was confirmed by an analysis of covariance (ANCOVA) with motion types as a between-subjects factor and density levels as a covariate. The main effect of motion types was found to be significant ($F(2, 101) = 11.94$, $p < .001$), meaning that the average thresholds for different motion types were significantly different after adjustment for density levels. In particular, the coherence threshold for translational motion (adjusted mean = 0.646) was found to be significantly different from those for circular (adjusted mean = 0.437, $F(1, 101) = 18.68$, $p < .001$) and radial motion (adjusted mean = 0.446, $F(1, 101) = 17.10$, $p < .001$), while that for circular motion was not significantly different from that for radial motion ($F(1, 101) = 0.035$, $p = .85$). This result reveals a "complexity advantage" for circular/radial motion over translational motion in terms of human sensitivity in perceiving global motion.[1]

In assessing how spatial density affected motion sensitivity, we found that threshold-density slopes were not significantly different across motion types ($F(2, 99) = 0.036$, $p = .97$). Furthermore, the ANCOVA analysis revealed a non-significant main effect of element density ($F(1, 101) = 0.061$, $p = .81$), indicating that the density slopes for all motion types were not significantly different from zero. This result implies that motion sensitivity varied very little with element density. The linear regression lines had mean slopes with 95% confidence interval as: -0.0045 ± 0.04 for translational motion, 0.0014 ± 0.02 for circular motion, and -0.0046 ± 0.05 for radial motion.

The results of Experiment 1 thus revealed lower motion sensitivity for translational than that for circular and radial motion. This finding suggests that specific motion integration mechanisms may operate for different motion types. Of particular interest is the counterintuitive observation that humans actually perform better in perceiving global circular/radial motion, motion types that have been considered more complex relative to translational motion. The results of Experiment 1 are consistent with those found by Freeman and Harris (1992) using the RDK stimulus. In terms of the effect of spatial density, the present findings are consistent with the results obtained using the RDK stimulus (Badcock & Khuu, 2001; Barlow & Tripathy, 1997; Edwards & Badcock, 1994, 1995,

1996; Morrone et al., 1995), as human observers yielded similar qualitative patterns of results when using the multiple-aperture stimuli. This agreement indicates that the visual system is able to pool motion information over broad ranges with constant efficiency in perceiving translational, circular, and radial motion. Nevertheless, the difference between simple translational motion and complex circular/radial motion remained across different density levels. In summary, the two findings, sensitivity difference across motion types and invariant sensitivity with element density, suggest that specialized integration mechanisms for the three motion patterns may share the same linear pooling principle as part of their computations.

Experiment 2: Effects of speed on motion sensitivity

To investigate the dependency of sensitivity on motion speed for the three types of global motion, we measured motion sensitivity at various speeds using the multiple-aperture stimulus. Early physiological studies have demonstrated the speed tuning of motion-sensitive neurons. Maunsell and Vanessen (1983) found that MT cells in macaque monkeys responded to specific ranges of speed. Tanaka and Saito (1989) found that MST cells sensitive to translational and radial motion showed speed selectivity with a narrow speed tuning function. However, about one third of circular sensitive MST cells showed the property of speed invariance with a flat speed tuning function. Consistent results were obtained in subsequent studies on cells in MST within a similar speed range (Orban, Lagae, Raiguel, Xiao, & Maes, 1995), particularly in the dorsal region MSTd (Duffy & Wurtz, 1997). Experiment 2 aimed to investigate the effect of speed on motion sensitivity within the range of 0.7–2.5 deg/s. Given the fixed stimulus size and spatial frequency used in Gabor elements in the present study, faster speed tends to create a percept of flicker and this generates an unstable motion percept. We therefore focused on a low speed range relative to those tested in previous studies (Burr, Morrone, & Vaina, 1998; Orban et al., 1995; Tanaka & Saito, 1989).

Methods

Subjects

A total of 102 undergraduate students at UCLA participated in this experiment for course credit. All observers were naïve to the purpose of the experiment and had normal or corrected-to-normal visual acuity. Thirty-four participants were randomly assigned to one of three speed conditions.

Stimulus

The stimuli used in Experiment 2 were similar to those used in Experiment 1 with the highest spatial density, i.e., 728 elements. However, the 2D motion speed was varied for each observer group. Three speed levels were used: 0.79 deg/s (same as that used in Experiment 1), 1.58 deg/s, and 2.37 deg/s. Speed was manipulated by changing the magnitude of phase shift of the Gabors per frame, so that the number of frames (and thus stimulus duration) remained the same as in Experiment 1.

Procedure

Observers performed the same global direction discrimination task as in Experiment 1. Each observer viewed motion stimuli for all three motion types but at one speed level. Observers first received a 60-trial practice session (20 trials for each motion type) to familiarize themselves with the stimulus and the task. Coherence ratio was decreased gradually from 100% to 90% over the 20 trials for each motion type. Participants were then presented with the experiment session, in which the three motion types were arranged in three blocks of 240 trials. The order of presentation of motion types was counterbalanced among observers. Each block started with on-screen instructions to inform observers of the motion type and response buttons for the upcoming block. In each block, participants were informed that the first 60 trials were practice for that particular type of motion. The remaining 180 trials were experiment trials, which were used to estimate coherence threshold via the QUEST adaptive-staircase procedure (Watson & Pelli, 1983). Participants were given negative feedback (a beep for error) in both practice and experiment trials, as in Experiment 1.

Results and discussion

Figure 8 shows that the coherence threshold for translational motion was higher than those for circular and radial motion when speed was the slowest (translational vs. circular, $F(1, 99) = 5.25$, $p = .02$; translational vs. radial, $F(1, 99) = 8.35$, $p = .01$), replicating the findings in Experiment 1. However, the difference between translational and radial motion was reduced as speed increased, although the thresholds for circular motion were nearly constant over the speed range tested in the experiment. A repeated-measures ANOVA with two factors (motion type as a within-subjects factor, speed as a between-subjects factor) was conducted to compare thresholds for different motion types at each speed level. This analysis revealed a significant main effect of motion type ($F(2, 198) = 23.88$, $p < .001$), indicating different sensitivity for the three motion types, which confirmed the general findings of Experiment 1. A significant interaction between motion

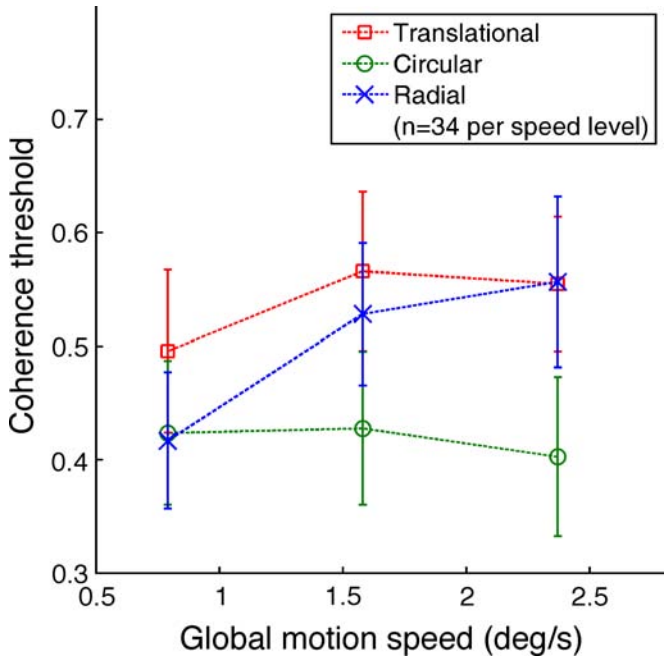

Figure 8. Results of Experiment 2. Coherence thresholds as a function of speeds. The figure shows the coherence thresholds (averaged across all observers) for translational (red open squares), circular (green open circles), and radial (blue crosses) motion. Error bars indicate the 95% confidence intervals for the estimates of the means.

type and speed was obtained ($F(4, 198) = 3.53$, $p = .01$), indicating that speed was an important factor influencing the sensitivity differences among motion types. Planned comparisons revealed how speed affects motion sensitivity for each specific motion type. In particular, global motion sensitivity for circular motion remained fairly constant across different speed levels ($F(2, 99) = 0.17$, $p = .85$), whereas sensitivity for radial motion was impaired as speed increased ($F(2, 99) = 4.80$, $p = .01$). A decreasing trend in sensitivity was also observed for translational motion as speed increased, although this trend fell short of statistical significance ($F(2, 99) = 1.39$, $p = .26$). These findings suggest that the integration mechanism specialized for circular motion may be tuned for a broad range of speeds. In contrast, radial motion integration mechanism may be more speed dependent. This implication is consistent with the physiological finding that a subgroup of circular MST cells (about one third of tested neurons) shows the speed-invariance characteristic, whereas most radial MST cells are speed selective (Tanaka & Saito, 1989).

Within the tested speed range, the complexity advantage effect for circular versus translational motion demonstrated robustness over the change of the speed. However, the effect for radial motion was speed dependent. From an ecological perspective, in natural scenes, radial motion is often associated with the observer's movements (ego-motion) under conditions rather different from those associated with translational and circular motion. In order to use the perceived optic flow to infer the observer's movement relative to the environment, the mechanisms for encoding radial motion need to be rather sensitive to speed change. As a result, speed change may affect human sensitivity for radial motion more than it does for circular motion. Tanaka and Saito (1989) showed that average responses of all circular-motion-selective cells increase as speed increases; a similar trend was also obtained for radial-motion-selective cells. However, the increase in slope for radial motion cells was much shaper than the increase in slope for circular motion cells, which is consistent with our finding of speed-dependent sensitivity for radial motion and speed-invariance sensitivity for circular motion.

Experiment 3: Time course of motion integration

Experiment 3 was designed to examine the temporal properties of motion integration mechanisms specialized for different motion types. Using random-dot stimuli, Burr and Santoro (2001) identified the "critical durations" needed for integrating different global motion patterns. Critical duration was defined as follows: If a motion stimulus is presented for a period of time that is shorter than the critical duration, motion sensitivity increases linearly with stimulus duration on a log–log scale; when the presentation time is longer than the critical duration, motion sensitivity remains constant when stimulus duration is further increased. Burr and Santoro (2001) used coherence threshold as the measure of motion sensitivity using the RDK stimulus. The investigators found that the global-motion integration stage needs long summation periods, about 3 seconds. In addition, their Experiment 2A revealed comparable critical durations for the three motion types. This result motivated us to conduct Experiment 3 using the multiple-aperture stimulus to examine the time course of integration for different motion types.

Methods

Subjects

Four observers (the first author and three naïve subjects) participated in this experiment. All observers had normal or corrected-to-normal visual acuity.

Stimulus

The stimuli were identical to those with the highest spatial density used in Experiment 1, except that the presentation time of the motion stimulus was manipulated. Fourteen different stimulus durations between 27 ms (two frames) and 413 ms (31 frames) were tested.

Procedure

Observers performed the same global direction discrimination task as in Experiment 1. Each observer viewed motion stimuli for all three motion types, with each motion type presented in a separate session. Observers were informed of which motion type they would be viewing in a particular session. The order of motion types were counterbalanced between observers. Before the start of each experiment session, observers were given 112 practice trials of the same motion type, with randomized stimulus durations (eight trials for each of the 14 stimulus durations). Coherence ratio was 100% for all practice trials. During the experiment session, observers completed a total of 1400 trials, with the order for the 14 durations

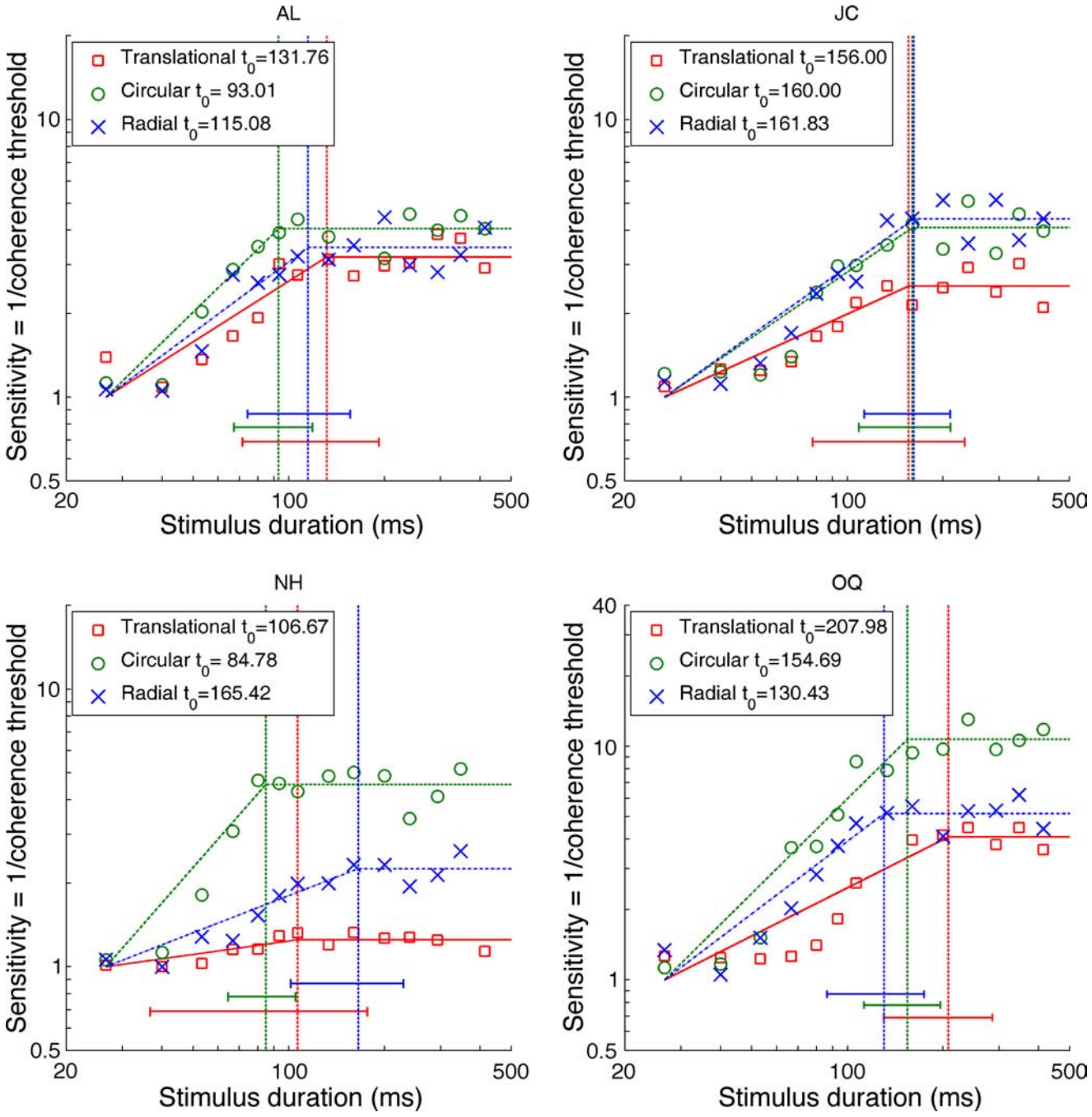

Figure 9. Results of Experiment 3. Motion sensitivity for each motion type (separate lines) as a function of stimulus duration for each observer (separate graphs). Motion sensitivities for translational, circular, and radial motion are plotted as red open squares, green open circles, and blue crosses, respectively. Each fitted line (translational: red solid; circular: blue dash-dot; radial: green dashed) shows the predicted sensitivity for each motion type using the fitted parameters. Vertical dashed lines mark the critical duration (estimate of t_0) for each motion type, and the horizontal error bars mark the 95% confidence intervals of the estimates in their corresponding colors.

randomized from trial to trial. QUEST adaptive-staircase procedure was used to estimate coherence thresholds for the 14 stimulus durations (100 trials for each duration). Participants were given negative feedback in both practice and experiment trials as in Experiments 1 and 2.

Results and discussion

Figure 9 depicts the results from four observers in Experiment 3. We performed an analysis similar to that conducted by Burr and Santoro (2001). Motion sensitivity was defined as the reciprocal of coherence threshold. Least-square regression was performed to estimate the parameters in the following equation for sensitivity (adopted from Burr & Santoro, 2001):

$$S = \begin{cases} S_0 \left(\frac{t}{t_0}\right)^p & \text{for } t \le t_0 \\ S_0 & \text{otherwise} \end{cases}, \quad (1)$$

where S indicates measured motion sensitivity and t indicates duration of motion stimulus. The parameters included p, the slope of the fitted line in a log–log coordinates; t_0, the critical duration for temporal integration; and S_0, a constant for motion sensitivity at the plateau level of performance. The three parameters were estimated using non-linear regression, with a constraint that the predicted sensitivity was greater than or equal to one (because the coherence ratio is bounded within a range of 1 to 0) for the shortest duration (i.e., 27 ms) in the experiment.

The three parameters were estimated for each motion type for each observer. Data points with standardized residual greater than or equal to two in the regression analysis were categorized as outliers. Based on this criterion, one data point was excluded in each of the regression analyses in the circular condition for observer AL, in the translational condition for observer OQ, and in all three motion conditions for observer NH. As shown in Table 1, the overall goodness of the fit, R^2 for the regressions was in the range from .71 to .92, with an average of .85. These findings indicate a reasonable quality of fit.

Table 1 shows the parameter estimates for each motion condition for each observer. We found that the estimated critical durations for temporal integration (t_0) for all motion types were short, around 140 ms. This result is not in agreement with the temporal limits reported by Burr and Santoro (2001), in which they found the critical durations for all motion types to be about 2–3 seconds (more than 10 times longer than the critical durations as revealed in the present study). This large discrepancy may be due to the use of different stimuli (multiple-aperture stimulus versus RDK stimulus) and experimental setups, a point to be taken up in the discussion. On the other hand, we found that critical durations were not significantly different for different motion types; the 95% confidence intervals of estimated critical durations for the three motion types overlapped for all observers, as shown in Figure 9. This result (invariance in the limit of temporal integration across motion types) was consistent with findings from the RDK experiment (Experiment 2A) reported by Burr and Santoro (2001). For the saturated range of duration (longer than critical duration), motion sensitivity for complex motion types (i.e., circular and radial) was found to be higher than that for translational motion, which again replicated the main findings from Experiments 1 and 2.

General discussion

The results of all three experiments reported in the present study demonstrate greater motion sensitivity in

Observer	Motion type	p	95% CI for p	t_0	95% CI for t_0	S_0	95% CI for S_0	R^2
AL	Translational	0.73	(0.24, 1.22)	131.76	(71.63, 191.88)	3.20	(2.86, 3.54)	0.82
	Circular	1.12	(0.47, 1.76)	93.01	(67.31, 118.71)	4.04	(3.72, 4.37)	0.90
	Radial	0.85	(0.29, 1.40)	115.08	(74.33, 155.82)	3.46	(3.05, 3.88)	0.79
JC	Translational	0.52	(0.20, 0.84)	156.00	(77.75, 234.25)	2.51	(2.25, 2.78)	0.81
	Circular	0.78	(0.41, 1.16)	160.00	(108.74, 211.26)	4.08	(3.55, 4.60)	0.86
	Radial	0.82	(0.45, 1.19)	161.83	(113.26, 210.40)	4.38	(3.84, 4.92)	0.88
NH	Translational	0.16	(0.03, 0.29)	106.67	(36.73, 176.61)	1.25	(1.19, 1.31)	0.71
	Circular	1.31	(0.48, 2.13)	84.78	(64.49, 105.07)	4.54	(4.08, 5.00)	0.87
	Radial	0.45	(0.26, 0.64)	165.42	(101.39, 229.44)	2.25	(2.03, 2.48)	0.88
OQ	Translational	0.69	(0.39, 0.98)	207.98	(130.17, 285.79)	4.09	(3.55, 4.64)	0.90
	Circular	1.35	(0.66, 2.04)	154.69	(113.04, 196.33)	10.70	(9.57, 11.84)	0.92
	Radial	1.03	(0.43, 1.64)	130.43	(86.36, 174.51)	5.15	(4.64, 5.66)	0.90

Table 1. Estimated parameters in regression analyses to describe human sensitivity as a function of stimulus duration. The parameters are p, the slope of the fitted line in a log–log coordinates; t_0, the critical duration for temporal integration; and S_0, a constant for motion sensitivity.

perceiving complex motion (i.e., circular and radial motion) than in perceiving translational motion, implying that different motion integration mechanisms are involved in the computation for different global motion patterns. This general finding is consistent with that reported by Freeman and Harris (1992) based on a study with the random-dot stimuli. Despite the difference between multiple-aperture stimuli used in the present study and the dot stimuli used by Freeman and Harris (1992), both studies were similar in using motion stimuli at relatively slow speed, which might be the reason that this complexity advantage was obtained in both studies. Furthermore, the qualitative patterns of the present results were also observed in studies using Glass patterns to investigate global form perception (Wilson & Wilkinson, 1998), in which observers were found to be more sensitive in detecting concentric and radial patterns than parallel patterns. As pointed out by Ross, Badcock, and Hayes (2000), form perception of Glass patterns might be closely related to motion perception of corresponding motion types at higher level of visual processing. Taken together with these studies, our findings provide converging evidence to support a complexity advantage in perceiving different types of motion patterns.

In contrast, Blake and Aiba (1998) did not find a significant difference in motion sensitivity for translational, circular, and radial motion. A possible account for this discrepancy could be the difference between the stimuli used in the two studies. Given their goal of studying general optic flow processing, Blake and Aiba (1998) used densely distributed dots moving against a bright background as motion stimuli, which produced correspondence noise (Barlow & Tripathy, 1997). From a computational perspective, correspondence noise introduces labeling uncertainty in determining which dot in one frame corresponds to which dot in the next frame (Barlow & Tripathy, 1997; Lu & Yuille, 2006). As a result, correspondence uncertainty directly affects the local velocity estimate of each dot and further influences the perceived global motion via spatial integration. However, given that 1D motion (component motion) is observable for the multiple-aperture stimulus used in the present study, the visual system needs to adopt an appropriate pooling strategy to integrate the observed 1D motion over space in order to infer the global motion. The inconsistency in findings between the present study and that of Blake and Aiba (1998) may thus reflect the fact that different stimuli produced uncertainty at different levels of motion processing.

Another discrepancy involving human performance when using the RDK stimuli compared to the multiple-aperture stimuli was revealed in Experiment 3. Whereas observers needed 2–3 seconds for temporal integration to perceive global motion displayed in the RDK stimulus (Burr & Santoro, 2001), the multiple-aperture stimulus yielded a much shorter period required for temporal integration, 100–200 ms. We suspect that different levels of uncertainty introduced by the two distinct stimuli could account for this large discrepancy. As each element in the multiple-aperture stimulus was a continuously drifting Gabor grating with medium contrast, local motion processors (such as motion energy detectors) could readily extract the component motion velocity (1D motion) for each element. In contrast, the RDK stimulus introduces large correspondence uncertainty in the estimation of the local velocity of each dot. Several studies have shown that the human visual system is not efficient in coping with this type of noise, as indicated by very low absolute efficiency value, less than 5% (Barlow & Tripathy, 1997; Lu & Yuille, 2006). Thus, the visual system needs more stimulus information, as is provided by longer duration, to perceive global motion displayed in the RDK stimulus.

Although humans showed shorter durations for temporal integration using the multiple-aperture stimulus than using the RDK stimulus, the absolute coherence thresholds (0.4–0.6) obtained in our study was much higher than the thresholds (0.05–0.15) that have been reported in most studies using the RDK stimulus. This discrepancy may be due to the use of local-tracking strategies, which may facilitate global motion perception for RDK stimuli in some studies. Also, in most previous studies observers were well trained and experienced participants in psychophysical experiments. The observers in our studies, junior undergraduate students who participated for course credit, were inexperienced and likely less motivated. Although we provided 70 practice trials before the experiment, naïve observers still produced much higher thresholds than experienced ones. In our pilot studies using experienced observers ($n = 7$), average discrimination thresholds for translational, circular, and radial motion were 0.35, 0.20, and 0.27, respectively. These values are about half of the thresholds obtained for naïve subjects. These results have been reported in abstract form (Lee, Yuille, & Lu, 2008). The differences in terms of subject population also contributed to the finding that thresholds in our studies were much higher than those found in previous studies by Amano et al. (2009) using the multiple-aperture stimulus in a large viewing window, which were in the range of 0.1–0.3. The fact that the complexity advantage is obtained even with naïve subjects indicates the robustness of the phenomenon.

In addition, three factors related to stimulus parameters may also have influenced the main findings in our study. First, eye movements may interfere with translational motion more than the other two complex motions, which might contribute to the complexity advantage found in our study. Although we cannot completely rule out this possibility, we believe the effect of eye movements was relatively small. Most of our stimuli had a brief presentation duration, around 260 ms (except the shortest was 27 ms and the longest was 413 ms in Experiment 3), minimizing the effect of eye movements. Also, all observers were given clear instructions to fixate the central dot throughout the session and had sufficient practice trials before they ran any experiment sessions.

A second possible concern involves the removal of speed gradient for circular and radial stimuli. Lack of speed gradient for the two complex motions leads to a percept of non-rigid rotation and expansion, which is inconsistent with optic flows observed in natural viewing situations. Although this is a very reasonable concern, this lack of naturalness may have placed the complex motion stimuli at a disadvantage for sensitivity and hence cannot explain the complexity advantage we obtained. In addition, we conducted a pilot study (reported in abstract form; Lee et al., 2008) that compared human sensitivity when viewing rigid (with speed gradient) and non-rigid (without speed gradient) movements for circular and radial motion using multiple-aperture stimuli.[2] We did not find any significant difference in motion sensitivity between rigid and non-rigid patterns. This finding is consistent with evidence from early physiological studies (e.g., Tanaka, Fukuda, & Saito, 1989), which found that speed gradient did not significantly affect responses of selected neurons in the MST area of macaque monkeys (neural responses were similar for motion patterns with and without speed gradient). Therefore, we chose to keep the 2D speed constant for all motion types so as to make our findings comparable with translation and with previous studies using the similar method (e.g., Burr & Santoro, 2001; Morrone et al., 1995).

A third possible explanation for the complexity advantage is that the difference in motion sensitivity between translational and radial motion might be related to the inward bias found by Edwards and Badcock (1993). Because the present study employed the two-alternative direction discrimination task, the higher sensitivity of radial motion might be due to the higher sensitivity of inward motion on half of the radial trials, with translational and the other outward half of radial motion having similar sensitivity. However, if this were the explanation, then such a difference in motion sensitivity between translational and radial motion would have been observed in previous studies using a similar task. In fact, findings from previous studies using a similar procedure (e.g., Aaen-Stockdale et al., 2007; Bertone & Faubert, 2003; Morrone et al., 1995) reveal no significant difference between translational and radial motion, suggesting that the inward bias does not account for the general effect. In summary, it does not seem likely that the complexity advantage observed in the present study can be largely attributed to any of the abovementioned experimental or procedural factors.

The key finding of the present study, the complexity advantage, may seem counterintuitive in that the visual system was found to perform better on a more complex task (circular or radial motion cannot be defined simply by a unidirectional motion flow across space, as is the case for translational motion). However, physiological studies suggest that several high level visual areas are involved in processing complex motion patterns, which may help increase motion sensitivity for circular/radial motion in behavioral tasks. Consistent with the ecological importance of perceiving circular and radial motion, early physiological studies (Duffy & Wurtz, 1991; Tanaka & Saito, 1989) found that some neurons in the MST region selectively respond to circular/radial patterns. Furthermore, other studies have identified neurons that respond specifically to rotational and expansion patterns in other brain areas responsible for high level processing. Sakata et al. (1994) found that some "rotation-sensitive" neurons in the posterior parietal (PP) area respond specifically to rotary movements of objects. Krekelberg, Dannenberg, Hoffmann, Bremmer, and Ross (2003) found that implied motion from dynamic Glass patterns (Ross et al., 2000) triggered responses in neurons in the high-level motion area superior temporal sulcus (STS). Wall and Smith (2008) identified the cingulate sulcus visual area (CSv) as a candidate region that seems to respond exclusively to expanding flow patterns that imply egomotion (but not to other expanding patterns that do not imply egomotion). Evidence from these studies supports the hypothesis that there exist high-level processing units tuned for circular or radial motion, which may provide a top–down influence that aids selection of an appropriate integration mechanism tailored to specific motion patterns in order to perceive global motion.

In addition to the involvement of high level visual areas in analyzing circular/radial motion patterns, more neural resources may be allocated to processing complex motion as opposed to simple translational motion within the MST area, which has long been recognized as the primary area for processing optic flow. For example, Tanaka and Saito (1989) clustered MST cells into three types of responsive groups: direction cells that selectively respond to one of *eight* translational directions; rotation cells that selectively respond to *two* directions (either a clockwise or counterclockwise rotation); and expansion/contraction cells that selectively response to *two* directions (either an expansion or contraction). Although the total number of cells appeared to be similar across the three clusters, the number of cells specifically selective to left or right motion was less than the number of cells selective to one direction in circular and radial motion (since the researchers used *eight* translational directions for their translational stimuli, but only *two* directions for their circular and radial motion stimuli). The similar argument could also apply to the study (Duffy & Wurtz, 1991), which used *four* translational directions and *two* directions for complex motion. If a population-encoding strategy were adopted for neuronal processing of optic flow analysis, the variance of averaged response from selective neurons would be reduced with an increase in the number of selective neurons. Accordingly, we conjecture that the involvement of more MST neurons selective to circular/radial motion might improve the signal-to-noise ratio in neural processing, which could increase behavioral sensitivity and thus lead to the complexity advantage reported in this paper.

Our main finding, the complexity advantage, refutes any model in which the same rules for integrating local velocity signals are used in performing motion analysis for different global motion patterns. Several studies have shown that a generic integration strategy, such as a slow-and-smooth prior, can predict human performance well for translational motion (Weiss, Simoncelli, & Adelson, 2002; Yuille & Grzywacz, 1988). However, Wu, Lu, and Yuille (2009) showed that the standard slow-and-smooth prior cannot be a universal integration strategy for other motion types. Instead, for circular and radial motions, registration of motion structure was required, which can be modeled by extending the smoothness term in the generic priors. In their model, the circular and radial smoothness priors do not include any information about the specific rotation/expansion center (analogous to the standard slow-and-smooth prior in which no specific global translational directions are encoded). Thus, the model does not deliberately include any bias favoring complex motions over simple translational motion. Nonetheless, simulations confirm that this model is able to select the most effective integration strategy based upon perceived motion information, and this choice in turn affects the estimation of motion flow. This model further predicts the complexity advantage observed in our study and provides a good correspondence with neural processors specialized for complex motion, as revealed in physiological studies.

In addition, due to the general preference for slow motion encoded by the slowness term in all three generic priors, Wu et al.'s (2009) model predicts a general trend of reduced sensitivity (i.e., higher coherence thresholds) with an increase of speed. This prediction is largely consistent with the finding that speed affected coherence thresholds, as shown in Experiment 2. The fact that the influence of speed varied for different motion types (as shown Figure 8) suggests that relative weights between slowness and smoothness in the three generic models may differ depending on specific motion types. Future computational studies are needed to verify this conjecture by comparing with natural statistics of translational, circular, and radial optic flow fields.

Acknowledgments

This research was supported by a grant from the National Science Foundation (NSF BCS-0843880) to HL and was presented at the Annual Meetings of the Vision Sciences Society, Naples, Florida, in 2007 and 2008. We thank Jonny Chan for his help in data collection.

Commercial relationships: none.
Corresponding author: Hongjing Lu.
Email: hongjing@ucla.edu.
Address: Department of Psychology, Franz Hall, UCLA, Los Angeles, CA 90095, USA.

Footnotes

[1]This "complexity advantage" was found to be robust over a range of contrasts. In our pilot study, we employed 100% density and four levels of contrasts, 0.05, 0.1, 0.2, and 0.4 to compare human sensitivity for the three motion types. All other stimulus parameters were the same as in Experiment 1. The "complexity advantage" of circular and radial motion over translational motion was consistently observed across the four contrast levels for all three subjects, with only one exception when contrast was 0.05 for Subject 3.

[2]Ten naïve subjects participated in this pilot study. Each observer participated in five blocks, including translational motion, circular motion with and without speed gradient, and radial motion with and without speed gradient. The other stimulus parameters and experimental procedures were the same as in Experiment 1, using the largest density level. We found no difference between rigid and non-rigid conditions. Thresholds were respectively 0.46 and 0.42 for the two conditions with circular motion, and 0.45 and 0.42 respectively with radial motion.

References

Aaen-Stockdale, C., Ledgeway, T., & Hess, R. F. (2007). Second-order optic flow processing. *Vision Research, 47,* 1798–1808. [PubMed]

Ahlstrom, U., & Borjesson, E. (1996). Segregation of motion structure from random visual noise. *Perception, 25,* 279–291. [PubMed]

Amano, K., Edwards, M., Badcock, D. R., & Nishida, S. (2009). Adaptive pooling of visual motion signals by the human visual system revealed with a novel multi-element stimulus. *Journal of Vision, 9*(3):4, 1–25, http://journalofvision.org/9/3/4/, doi:10.1167/9.3.4. [PubMed] [Article]

Badcock, D. R., & Khuu, S. K. (2001). Independent first and second-order motion energy analyses of optic flow. *Psychological Research, 65,* 50–56. [PubMed]

Barlow, H., & Tripathy, S. P. (1997). Correspondence noise and signal pooling in the detection of coherent visual motion. *Journal of Neuroscience, 17,* 7954–7966. [PubMed] [Article]

Beardsley, S. A., & Vaina, L. A. (2005). Psychophysical evidence for a radial motion bias in complex motion discrimination. *Vision Research, 45,* 1569–1586. [PubMed]

Bertone, A., & Faubert, J. (2003). How is complex second-order motion processed? *Vision Research, 43,* 2591–2601. [PubMed]

Bex, P. J., Metha, A. B., & Makous, W. (1999). Enhanced motion aftereffect for complex motions. *Vision Research, 39,* 2229–2238. [PubMed]

Blake, R., & Aiba, T. S. (1998). Detection and discrimination of optical flow components. *Japanese Psychological Research, 40,* 19–30.

Brainard, D. H. (1997). The psychophysics toolbox. *Spatial Vision, 10,* 433–436. [PubMed]

Britten, K. H., Shadlen, M. N., Newsome, W. T., & Movshon, J. A. (1993). Responses of neurons in macaque MT to stochastic motion signals. *Visual Neuroscience, 10,* 1157–1169. [PubMed]

Burr, D. C., Badcock, D. R., & Ross, J. (2001). Cardinal axes for radial and circular motion, revealed by summation and by masking. *Vision Research, 41,* 473–481. [PubMed]

Burr, D. C., Morrone, M. C., & Vaina, L. M. (1998). Large receptive fields for optic flow detection in humans. *Vision Research, 38,* 1731–1743. [PubMed]

Burr, D. C., & Santoro, L. (2001). Temporal integration of optic flow, measured by contrast and coherence thresholds. *Vision Research, 41,* 1891–1899. [PubMed]

Clifford, C. W. G., Beardsley, S. A., & Vaina, L. M. (1999). The perception and discrimination of speed in complex motion. *Vision Research, 39,* 2213–2227. [PubMed]

Duffy, C. J., & Wurtz, R. H. (1991). Sensitivity of MST neurons to optic flow stimuli: I. A continuum of response selectivity to large-field stimuli. *Journal of Neurophysiology, 65,* 1329–1345. [PubMed] [Article]

Duffy, C. J., & Wurtz, R. H. (1997). Medial superior temporal area neurons respond to speed patterns in optic flow. *Journal of Neuroscience, 17,* 2839–2851. [PubMed] [Article]

Edwards, M., & Badcock, D. R. (1993). Asymmetries in the sensitivity to motion in depth: A centripetal bias. *Perception, 22,* 1013–1023. [PubMed]

Edwards, M., & Badcock, D. R. (1994). Global motion perception—Interaction of the on and off pathways. *Vision Research, 34,* 2849–2858. [PubMed]

Edwards, M., & Badcock, D. R. (1995). Global motion perception—No interaction between the first-order and 2nd-order motion pathways. *Vision Research, 35,* 2589–2602. [PubMed]

Edwards, M., & Badcock, D. R. (1996). Global-motion perception: Interaction of chromatic and luminance signals. *Vision Research, 36,* 2423–2431. [PubMed]

Emerson, R. C., Bergen, J. R., & Adelson, E. H. (1992). Directionally selective complex cells and the computation of motion energy in cat visual cortex. *Vision Research, 32,* 203–218. [PubMed]

Freeman, T. C. A., & Harris, M. G. (1992). Human sensitivity to expanding and rotating motion—Effects of complementary masking and directional structure. *Vision Research, 32,* 81–87. [PubMed]

Heeger, D. J., Simoncelli, E. P., & Movshon, J. A. (1996). Computational models of cortical visual processing. *Proceedings of the National Academy of Sciences of the United States of America, 93,* 623–627. [PubMed] [Article]

Krekelberg, B., Dannenberg, S., Hoffmann, K. P., Bremmer, F., & Ross, J. (2003). Neural correlates of implied motion. *Nature, 424,* 674–677. [PubMed]

Lee, A. L-f., Yuille, A., & Lu, H. (2008). Superior perception of circular/radial than translational motion cannot be explained by generic priors [Abstract]. *Journal of Vision, 8*(6):31, 31a, http://journalofvision.org/8/6/31/, doi:10.1167/8.6.31.

Lu, H., & Yuille, A. L. (2006). Ideal observers for detecting motion: Correspondence noise. In B. Schölkopf, J. Platt, & T. Hofmann (Eds.), *Advances in neural information processing systems* (vol. 18, pp. 827–834). Cambridge, MA: MIT Press. [Article]

Maunsell, J. H. R., & Vanessen, D. C. (1983). Functional-properties of neurons in middle temporal visual area of the macaque monkey: I. Selectivity for stimulus direction, speed, and orientation. *Journal of Neurophysiology, 49,* 1127–1147. [PubMed]

Mingolla, E., Todd, J. T., & Norman, J. F. (1992). The perception of globally coherent motion. *Vision Research, 32,* 1015–1031. [PubMed]

Morrone, M. C., Burr, D. C., & Vaina, L. M. (1995). Two stages of visual processing for radial and circular motion. *Nature, 376,* 507–509. [PubMed]

Orban, G. A., Lagae, L., Raiguel, S., Xiao, D. K., & Maes, H. (1995). The speed tuning of medial superior temporal (MST) cell responses to optic-flow components. *Perception, 24,* 269–285. [PubMed]

Pelli, D. G. (1997). The VideoToolbox software for visual psychophysics: Transforming numbers into movies. *Spatial Vision, 10,* 437–442. [PubMed]

Ross, J., Badcock, D. R., & Hayes, A. (2000). Coherent global motion in the absence of coherent velocity signals. *Current Biology, 10,* 679–682. [PubMed]

Rust, N. C., Mante, V., Simoncelli, E. P., & Movshon, J. A. (2006). How MT cells analyze the motion of visual patterns. *Nature Neuroscience, 9,* 1421–1431. [PubMed] [Article]

Sakata, H., Shibutani, H., Ito, Y., Tsurugai, K., Mine, S., & Kusunoki, M. (1994). Functional-properties of rotation-sensitive neurons in the posterior parietal association cortex of the monkey. *Experimental Brain Research, 101,* 183–202. [PubMed]

Tanaka, K., Fukada, Y., & Saito, H. A. (1989). Underlying mechanisms of the response specificity of expansion contraction and rotation cells in the dorsal part of the medial superior temporal area of the macaque monkey. *Journal of Neurophysiology, 62,* 642–656. [PubMed]

Tanaka, K., & Saito, H. A. (1989). Analysis of motion of the visual-field by direction, expansion contraction, and rotation cells clustered in the dorsal part of the medial superior temporal area of the macaque monkey. *Journal of Neurophysiology, 62,* 626–641. [PubMed]

Wall, M. B., & Smith, A. T. (2008). The representation of egomotion in the human brain. *Current Biology, 18,* 191–194. [PubMed]

Watson, A. B., & Pelli, D. G. (1983). Quest: A Bayesian adaptive psychometric method. *Perception & Psychophysics, 33,* 113–120. [PubMed]

Weiss, Y., Simoncelli, E. P., & Adelson, E. H. (2002). Motion illusions as optimal percepts. *Nature Neuroscience, 5,* 598–604. [PubMed] [Article]

Wilson, H. R., & Wilkinson, F. (1998). Detection of global structure in Glass patterns: Implications for form vision. *Vision Research, 38,* 2933–2947. [PubMed]

Wu, S., Lu, H., & Yuille, A. L. (2009). Model selection and parameter estimation in motion perception. In D. Koller, D. Schuurmans, Y. Bengio, & L. Bottou (Eds.), *Advances in neural information processing systems* (vol. 21, pp. 1793–1800). Cambridge, MA: MIT Press. [Article]

Yuille, A. L., & Grzywacz, N. M. (1988). A computational theory for the perception of coherent visual-motion. *Nature, 333,* 71–74. [PubMed]